

# DEM extraction and its accuracy analysis with ground-based SAR interferometry

J Dong<sup>1</sup>, J P Yue<sup>1,3</sup> and L H Li<sup>2</sup>

<sup>1</sup>School of Earth Science and Engineering, Hohai University, Nanjing, 210098, China.

<sup>2</sup>School of Land Science and Technology, China University of Geosciences (Beijing), Beijing, 100083, China.

jaydowhhu@126.com; jpyue@hhu.edu.cn; lilihua992@163.com

**Abstract.** Two altimetry models extracting DEM (Digital Elevation Model) with the GBSAR (Ground-Based Synthetic Aperture Radar) technology are studied and their accuracies are analyzed in detail. The approximate and improved altimetry models of GBSAR were derived from the spaceborne radar altimetry based on the principles of the GBSAR technology. The error caused by the parallel ray approximation in the approximate model was analyzed quantitatively, and the results show that the errors cannot be ignored for the ground-based radar system. For the improved altimetry model, the elevation error expression can be acquired by simulating and analyzing the error propagation coefficients of baseline length, wavelength, differential phase and range distance in the mathematical model. By analyzing the elevation error with the baseline and range distance, the results show that the improved altimetry model is suitable for high-precision DEM and the accuracy can be improved by adjusting baseline and shortening slant distance.

**Keywords.** Ground-based Synthetic Aperture Radar (GBSAR) Interferometry, DEM, Altimetry Model, Accuracy Analysis

## 1. Introduction

Synthetic aperture radar interferometry (InSAR) is one of the hottest fields of radar remote sensing. Ever since Zebker published the experimental DEM of San Francisco Bay Area extracted by the airborne InSAR system in 1986<sup>[1]</sup>, many scholars began to research InSAR in depth. Currently, the spaceborne radar altimetry can acquire a large amount of information of the illuminated area with low cost<sup>[2]</sup>. The surface and surrounding environment of interested area may change a lot during the satellite revisit interval, and these changes will result in low signal correlation. However, the ground-based SAR technology can survey the target area continuously with a shorter interval and overcomes the disadvantage of serious loss of space-time correlation with high space-time resolution.

GBSAR is an innovative microwave interferometry based on the same principles of satellite SAR<sup>[3-4]</sup>. The IBIS (Image by Interferometric Survey) telemetry system, the fruit of a long-term research activity performed in collaboration by IDS (Ingegneria dei Sistemi) and the University of Florence, Italy, has two types of IBIS-L and IBIS-S. Among them, The IBIS-L system has been used widely for monitoring landslides<sup>[5]</sup>, glaciers<sup>[6]</sup>, buildings<sup>[7]</sup>, and dams<sup>[8]</sup> with satisfied results. Nevertheless, it is

<sup>3</sup> J P Yue is the correspondence author.

The authors acknowledge the support of the National Natural Science Foundation of China (project grant no.: 41174002).



not mature for GBSAR to map topography<sup>[9]</sup>.

The approximate altimetry model of GBSAR is derived from the spaceborne radar altimetry on the condition of parallel ray approximation. This approximate altimetry model is exactly the same as the model presented by Noferini<sup>[9]</sup>. But accuracy analysis shows that this model has large error and is not suitable for high-precision DEM extraction. Therefore, the improved altimetry model should be obtained with the true range distance. Simulation analysis is applied to this improved model and some methods improving the accuracy are gotten.

## 2. The altimetry model of GBSAR

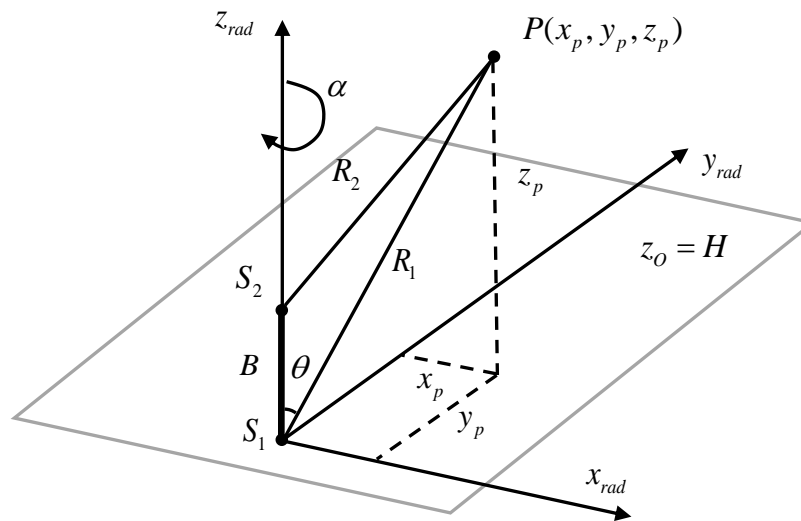


**Figure 1.** The altimetry geometry of GBSAR

The altimetry mechanism of GBSAR is similar to spaceborne SAR, but with some differences. The rail of IBIS-L system needs to be installed in a stable concrete pier. Horizontal sliding of the sensor on the rail forms a synthetic aperture and vertical lifting of the rail constitutes a baseline, which's horizontal component is zero. Figure 1 shows the geometry of GBSAR altimetry by taking point  $P(x_p, y_p, z_p)$  as an example. The system sensor scans the target area at the baseline ends of  $S_1$  and  $S_2$ . The axis  $x_{rad}$  of the Cartesian coordinate system is parallel to the rail; the axis  $y_{rad}$  is perpendicular to the rail; the axis  $z_{rad}$  is parallel to the vertical line and crosses the middle of the rail; and the origin  $(x_o, y_o, z_o) = (0, 0, H)$ ,  $H$  is the elevation of the sensor center at position  $S_1$ .  $R_1$  and  $R_2$  are range distances, the zenith of  $R_1$  is  $\theta$ , then:

$$z_p = R_1 \cos \theta \quad (1)$$

The conversion of differential phase to range difference:

$$\Delta R = R_1 - R_2 = \frac{\lambda \phi}{4\pi} \quad (2)$$

It is obtained according to the law of cosines in  $\Delta S_1 S_2 P$ :

$$R_2^2 = R_1^2 + B^2 - 2R_1 B \cos \theta \quad (3)$$

The range distance difference  $\Delta R$  approximates the projection of baseline in the direction of the range distance according to the parallel ray approximation method proposed by Zebker in airborne

radar altimetry<sup>[1]</sup>:

$$\Delta R \approx B \cos \theta \quad (4)$$

The approximate altimetry model is obtained from equation (1), (2) and (4):

$$h_p = H + \frac{\lambda \phi R_1}{4\pi B} \quad (5)$$

The true value of range distance difference can be gotten from equations (2) and (3):

$$\Delta R = \frac{\lambda^2 \phi^2}{32\pi^2 R_1} - \frac{B^2}{2R_1} + B \cos \theta \quad (6)$$

The elevation error  $\varepsilon_{h_p}$  caused by the approximation method can be solved from equations (4), (5) and (6):

$$\varepsilon_{h_p} = \frac{B}{2} - \frac{\lambda^2 \phi^2}{32\pi^2 B} \quad (7)$$

The center frequency ( $f_{cen} = 5.93GHz$ ) used in reference [9] infers corresponding wavelength  $\lambda = 5.059cm$ . The curves of elevation error to baseline with different differential phases are drawn in figure 2. The coincidence of the four curves indicates that elevation error has little relationship with differential phase; but it rises continually with baseline increasing and reaches maximum 0.25m when the baseline is 0.5m. So the elevation error caused by the approximate method can not be ignored. The improved altimetry model of GBSAR with the true range distance will be presented below.

The improved altimetry model can be derived from equations (1), (2) and (6):

$$h_p = H + \frac{B}{2} + \frac{\lambda \phi R_1}{4\pi B} - \frac{\lambda^2 \phi^2}{32\pi^2 B} \quad (8)$$

From the equation above, the elevation accuracy is related with the errors of sensor elevation, baseline length, radar wavelength, range distance and phase noise. It is of great significance to analyze the impacts of these terms on the elevation.

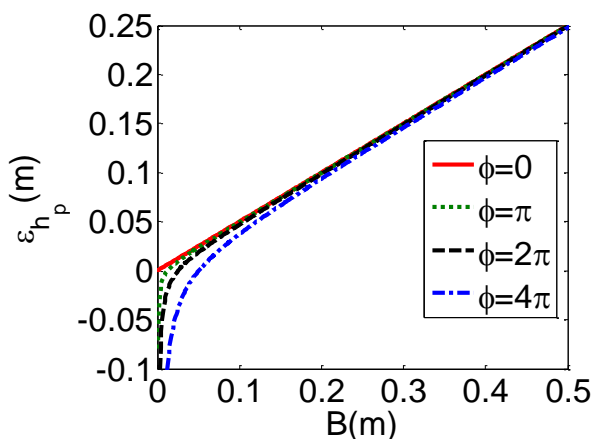


**Figure 2.** The elevation errors caused by approximation method.

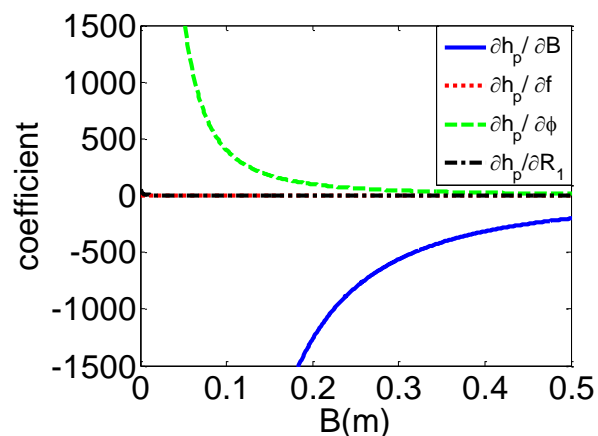


**Figure 3.** The curves of error propagation coefficients: the solid line represents baseline length; the dotted line represents frequency; the dashed line represents differential phase; the dash-and-dot line represents

range distance.

### 3. Accuracy analysis

Hereinafter, the accuracy of improved altimetry model will be analyzed in detail. The differential of equation (8) is:

$$dh_p = \begin{bmatrix} 1 & \frac{16\pi^2 B^2 + \lambda^2 \phi^2 - 8\pi\lambda\phi R_1}{32\pi^2 B^2} & \frac{4\pi\phi R_1 - \phi^2 \lambda}{16\pi^2 B^2} & \frac{4\pi\lambda R_1 - \lambda^2 \phi}{16\pi^2 B^2} & \frac{\lambda\phi}{4\pi B} \end{bmatrix} \begin{bmatrix} dH & dB & d\lambda & d\phi & dR_1 \end{bmatrix}^T \quad (9)$$

The elevation variance can be solved according to the variance propagation law if the elements are independent of each other:

$$\sigma_{h_p}^2 = \left(\frac{\partial h_p}{\partial H} \sigma_H\right)^2 + \left(\frac{\partial h_p}{\partial B} \sigma_B\right)^2 + \left(\frac{\partial h_p}{\partial \lambda} \sigma_\lambda\right)^2 + \left(\frac{\partial h_p}{\partial \phi} \sigma_\phi\right)^2 + \left(\frac{\partial h_p}{\partial R_1} \sigma_{R_1}\right)^2 \quad (10)$$

The error propagation coefficients are as follows:

$$\frac{\partial h_p}{\partial H} = 1 \quad (11)$$

$$\frac{\partial h_p}{\partial B} = \frac{16\pi^2 B^2 + \lambda^2 \phi^2 - 8\pi\lambda\phi R_1}{32\pi^2 B^2} \quad (12)$$

$$\frac{\partial h_p}{\partial \lambda} = \frac{4\pi\phi R_1 - \phi^2 \lambda}{16\pi^2 B^2} \quad (13)$$

$$\frac{\partial h_p}{\partial \phi} = \frac{4\pi\lambda R_1 - \lambda^2 \phi}{16\pi^2 B^2} \quad (14)$$

$$\frac{\partial h_p}{\partial R_1} = \frac{\lambda\phi}{4\pi B} \quad (15)$$

The frequency fluctuation of electromagnetic wave emitted by the system causes the change of wavelength, and the relationship between wavelength and frequency is:

$$\lambda = \frac{c}{f} \quad (16)$$

Consequently, the error propagation coefficient of wavelength can be replaced by the error propagation coefficient of frequency:

$$\frac{\partial h_p}{\partial f} = \frac{-4\pi\phi R_1 c + \phi^2 \lambda c}{16\pi^2 B^2 f^2} \quad (17)$$

By equation (11), the error propagation coefficient of sensor elevation is constant 1, i.e. the elevation measurement error of sensor participates in the target elevation equally.

The curves of the error propagation coefficients of baseline length, frequency, differential phase and range distance are simulated by computer under the conditions of  $R_1 = 1000m$ ,  $\phi = 4\pi$ ,  $c = 3.0 \times 10^8 m/s$ ,  $f = 5.93GHz$ , as shown in Figure 3.

The error propagation coefficients of frequency and range distance are very close to zero and do not change obviously when the baseline is increased. So the errors of frequency and range distance

will be reduced greatly during transfer process and can be ignored.

The error propagation coefficient of baseline decreases with baseline increasing. Tiny error of baseline length will be enlarged 200 times even when the coefficient reaches the minimum. Therefore, the measurement accuracy of baseline plays an important role in elevation accuracy.

The error propagation coefficient of differential phase decreases rapidly with the baseline increasing. The variation trend of the curve becomes gentle when the baseline reaches a value, however, this coefficient can not be ignored.

From the analyses above, the impacts of the errors of wavelength and range distance can be ignored. The measurement error of sensor elevation is an external factor and not concerned here. So the elevation error related to the errors of baseline length and differential phase can be expressed as:

$$\sigma_{h_p} = \sqrt{\left(\frac{16\pi^2 B^2 + \lambda^2 \phi^2 - 8\pi\lambda\phi R_1}{32\pi^2 B^2} \sigma_B\right)^2 + \left(\frac{4\pi\lambda R_1 - \lambda^2 \phi}{16\pi^2 B^2} \sigma_\phi\right)^2} \quad (18)$$

The DEM accuracy can be improved by studying the relationships of elevation error with baseline and range distance. Let baseline error  $\sigma_B = 0.001m$ , differential phase error  $\sigma_\phi = 0.5rad$ , wavelength  $\lambda = 5.059cm$  and differential phase  $\phi = 4\pi$  by referring to the reference [10].

The variation curve of elevation error with baseline is drawn from equation (18) when  $R_1 = 1000m$  (as shown in figure 4 (a)). The error curve declines from sharply to gently. So the elevation accuracy can be improved by enlarge the baseline in a certain extent. However large baseline will cause geometric decorrelation. So it is necessary to find an optimal baseline to make a trade-off between the minimized impact of baseline error and good correlation.

The variation curve of elevation error with range distance is drawn in figure 4 (b) when  $B = 0.5m$ . The elevation error increases linearly with range distance. The error of target point farther from the IBIS system is larger. For example, the error at the range distance 3000m doubles the error at 1500m. So the place installing the IBIS system should be chosen near the target area as far as possible in order to reduce elevation error.

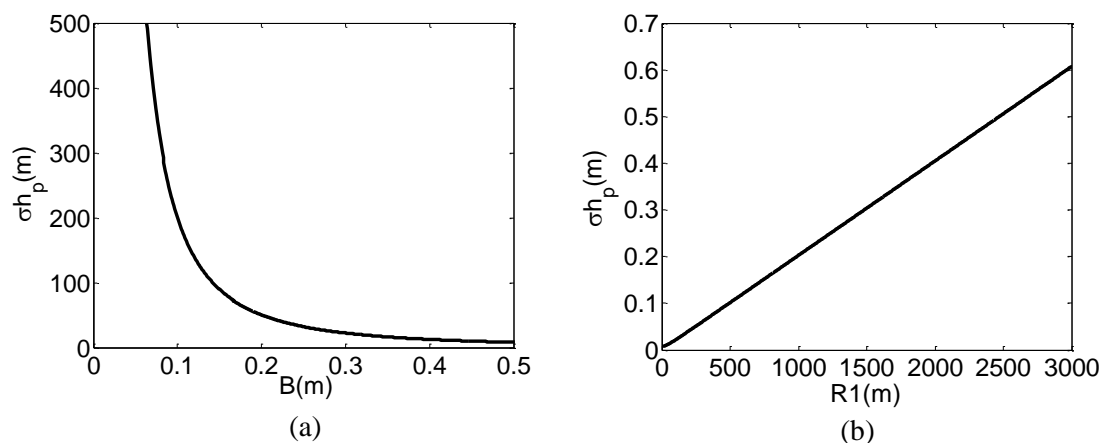


**Figure 4.** The curves of elevation error: (a) the curve of elevation error with baseline; (b) the curve of elevation error with range distance

#### 4. Conclusion

This paper presented the approximate and improved altimetry models of GBSAR derived from the spaceborne radar altimetry. The parallel ray approximation method in the approximate model introduces large error and it is unsuitable for high-precision DEM extraction. The simulation results of the error propagation coefficients in the improved altimetry model show that the baseline and differential phase are the main factors affecting the elevation accuracy. The analyses of the error

curves of elevation with baseline and range distance prove that enlarging the baseline or reducing the range distance can improve the model accuracy obviously. The specific selection criteria of the optimal baseline and atmospheric effect should be focused in the future study.

## References

- [1] Zebker H A and Goldstein R M Topographic mapping from interferometric synthetic aperture radar observations 1986 *J. geophys. Res.* **91** 4993-99
- [2] Bürgmann R, Rosen P A and Fielding E J Synthetic aperture radar interferometry to measure Earth's surface topography and its deformation 2000 *Annual Review of Earth and Planetary Sciences* **28** 169-209
- [3] Rosen P A, Hensley S, Joughin I R, Li F K, Madsen S N, Rodriguez E and Goldstein R M Synthetic aperture radar interferometry 2000 *Proceedings of the IEEE* **88** 333-82
- [4] Rodriguez E and Martin J M Theory and design of interferometric synthetic aperture radars 1992 *Radar and Signal Processing* **139** 147-59
- [5] Noferini L, Pieraccini M, Mecatti D, Macaluso G, Atzeni C, Mantovani M, Marcato G, Pasuto A, Silvano S and Tagliavini F Using GB-SAR technique to monitor slow moving landslide 2007 *Engineering Geology* **95** 88-98
- [6] Luzi G, Pieraccini M, Mecatti D, Noferini L, Macaluso G, Tamburini A and Atzeni C Monitoring of an Alpine glacier by means of ground-based SAR interferometry 2007 *IEEE Geoscience and Remote Sensing Letters* **4** 495-99
- [7] Pieraccini M, Tarchi D, Rudolf H, Leva D, Luzi G and Atzeni C Interferometric radar for remote monitoring of building deformations 2000 *Electronics Letters* **36** 569-70
- [8] Tarchi D, Rudolf H, Luzi G, Chiarantini L, Coppo P and Sieber A J 1999 SAR interferometry for structural changes detection: a demonstration test on a dam *Proceedings of IEEE International Geoscience and Remote Sensing Symposium* vol **3** (Hamburg: IEEE) p 1522-24
- [9] Noferini L, Pieraccini M, Mecatti D, Macaluso G, Luzi G and Atzeni C DEM by Ground-based SAR interferometry 2007 *IEEE Geoscience and Remote Sensing Letters* **4** 659-63
- [10] Nico G, Leva D, Antonello G and Tarchi D Ground-based SAR interferometry for terrain mapping: theory and sensitivity analysis 2004 *IEEE Transactions on Geoscience and Remote Sensing* **42** 1344-50